Simulated variability in the mean atmospheric meridional circulation over the 20th century

Damianos F. Mantsis[1] and Amy C. Clement[1]

Received 20 November 2008; revised 15 January 2009; accepted 22 January 2009; published 21 March 2009.

[1] The variability in the zonally averaged atmospheric meridional circulation over the last 150 years is investigated using two atmospheric general circulation models (GCMs). A multi-decadal signal, with an approximately 70 year timescale, is identified in the cross-equatorial circulation. This signal is associated with a latitudinal shift in the ascending branch of the Hadley cell and precipitation in the tropics, as well as a change in the atmospheric meridional heat transport. These changes are well-correlated with the inter-hemispheric SST difference: When Northern Hemisphere sea surface temperatures (SSTs) are colder than the Southern Hemisphere, the ITCZ and precipitation shift to the south in a zonal mean sense, and the northward atmospheric energy transport increases. Previous studies with idealized climate forcings have shown similar results, but the findings presented here highlight the potential relevance of the inter-hemispheric SST contrast for understanding 20th century climate changes.
Citation: Mantsis, D. F., and A. C. Clement (2009), Simulated variability in the mean atmospheric meridional circulation over the 20th century, *Geophys. Res. Lett.*, *36*, L06704, doi:10.1029/2008GL036741.

1. Introduction

[2] The primary reason the ocean-atmosphere system is in constant motion is to transport heat from low latitudes where there is a net radiative gain, to high latitudes where there is a net loss [*Trenberth and Caron*, 2001]. Seasonally, as one hemisphere gains more heat, the atmospheric response to this inter-hemispheric radiative contrast is a strengthening and expansion of the Hadley circulation of the colder hemisphere and a shift in the ITCZ toward the warmer hemisphere. This increases the cross-equatorial atmospheric heat transport from the warmer toward the colder hemisphere in order to satisfy the radiative loss. Modeling studies have shown that a similar phenomenon takes place on decadal to glacial-interglacial timescales in response to climate forcings that introduce inter-hemispheric radiative contrast, such as Northern Hemisphere continental ice, Northern Hemisphere sea-ice, changes in Atlantic thermohaline circulation and anthropogenic aerosols [*Chiang et al.*, 2003; *Chiang and Bitz*, 2005; *Broccoli et al.*, 2006; *Zhang and Delworth*, 2005; *Yoshimori and Broccoli*, 2008]. Here we test whether similar phenomena can operate in the 20th century climate by analyzing simulations of atmospheric GCMs forced by observed SST variations going back to the second half of the 19th century.

2. Model Simulations and Analysis

2.1. Model Simulations

[3] For this study we use two atmospheric GCMs, the Geophysical Fluid Dynamics Laboratory model (GFDL AM2.1) and the Community Climate Model version 3 (CCM3), *Kiehl et al.* [1998]. Both models are forced with observed SSTs from the second half of the 19th century to the end of the 20th century. For the CCM3 model we used 16-member ensemble that cover the period 1856–2004. The details of these simulations are given by *Seager et al.* [2005]. For the GFDL model we used a 20-member ensemble that covers the period 1870–2004. In ten of these ensemble members, climate forcings (i.e. CO_2, aerosols, solar irradiance) are held at constant values, and in the other ten they vary with time over the 20th century as in the IPCC simulations. The details of this model are given by *The GFDL Global Atmospheric Model Development Team* [2004].

2.2. Methodology

[4] We analyze the cross-equatorial component of the circulation, and as an index we use the zonal mean cross-equatorial meridional wind, averaged in the lower troposphere (1000–850hPa) from 20°S to 20°N (hereafter V-index). This index is highly correlated (above 0.9, significant to 99% level) with the first principal component of the time evolution of the zonal mean meridional streamfunction, and hence represents the dominant mode of variability of the meridional circulation. Other diagnostics used are the zonal average meridional streamfunction, calculated by vertically integrating the zonally averaged mass weighted v-wind [*Oort and Yienger*, 1996], ω-velocity and precipitation. The meridional heat transport of the ocean-atmosphere system is also used and is calculated from spherical integration of radiative fluxes at the TOA. In the same way the "implied" meridional ocean heat transport is calculated from sea surface fluxes, and the atmospheric heat transport is computed as the difference of these two [*Trenberth and Caron*, 2001].

[5] In order to separate the multidecadal component from the total variability a 16-year low pass Butterworth digital filter was applied, and the inter-annual/decadal component of the variability was calculated as the difference of the original and the filtered time-series. A similar analysis is applied on the multidecadal, the inter-annual/decadal as well as the total component, but only the results for the last one are shown. All of the following analysis is applied for annual mean conditions. Parts of this analysis is also applied to ERA40 [*Uppala et al.*, 2004] and NCEP1

[1]Rosenstiel School of Marine and Atmospheric Sciences, University of Miami, Miami, Florida, USA.

0094-8276/09/2008GL036741

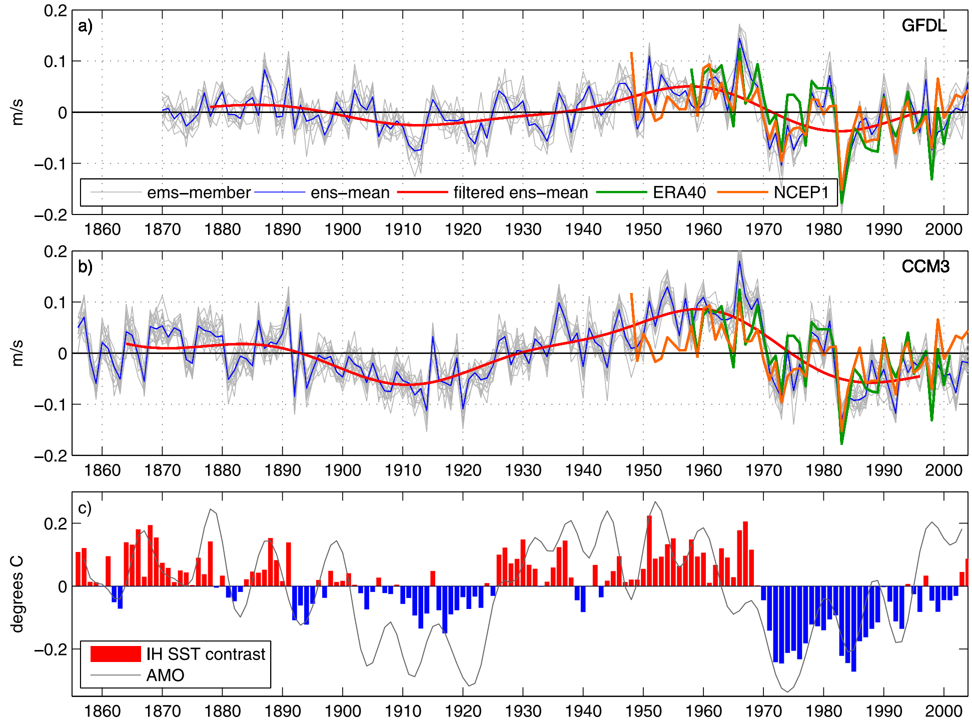

Figure 1. (a)–(b) Temporal variability of the cross-equatorial surface meridional wind anomaly. Displayed are the indices for each individual ensemble run, ensemble mean, 16-year low pass filtered ensemble mean for the two models, ERA40 and NCEP1 reanalysis datasets. (c) Inter-hemispheric SST difference, calculated from 60°S to 60°N, and 3-year low pass filtered AMO index (the area weighted average over the N. Atlantic, from 0° to 70°N, from http://www.cdc.noaa.gov/Timeseries/AMO/). The AMO index has been detrended and filtered in order to reduce its variability and make the comparison easier.

[*Kalnay et al.*, 1996] reanalysis datasets in order to validate the model results.

3. Results

[6] The analysis reveals that the zonal mean cross-equatorial wind anomaly exhibits variability on both multi-decadal (with an approximately 70 year period) and inter-annual/decadal timescales, in both models (Figure 1). The first order features of the evolution of the V-index are the positive phases that cover the period 1930–1970 as well as the first decades of the record, and indicate increased southerly trade winds across the equator. Similarly, the negative phases cover the first decades of the 20th century as well as the period 1970–2004, and indicate increased northerly trade winds across the equator. These signals appear not only in the ensemble mean but in individual ensembles of both models as well, which indicates the strong influence of the SST forcing. Furthermore, the variability of the cross-equatorial surface winds of the two models closely fallows those of ERA40 and NCEP1 reanalysis datasets, with a correlation above 0.63 (significant at the 99% confidence level).

[7] In order to diagnose the changes in the atmospheric circulation that are associated with the variability of the zonal mean cross-equatorial wind anomaly, regressions of the zonal mean meridional streamfunction, precipitation and ω-velocity on the V-index are shown in Figure 2. With a negative change in the V-index (hence anomalous northerly winds across the equator at the surface), there is anomalous ascending motion from 20°S to 2°N (Figures 2a–2b), and anomalous subsidence from 2°N to 20°N (results significant at 95% level of confidence using a student t-test). This reorganization of the zonal mean meridional overturning in the tropical region is associated with the development of a clockwise anomalous Hadley circulation centered just north of the equator (Figures 2c–2d), significant at 99% level. This reorganization is also seen in the ERA40 and NCEP1 reanalysis datasets and validates even more the results seen in the two models (not shown). These changes in the circulation, also lead to an increase in the tropical precipitation south of the equator and a decrease north of it (Figure 2e), indicating a shift in the ITCZ towards the warmer hemisphere (significant at 95% level). An EOF analysis applied to the zonal mean meridional streamfunction, revealed that the dominant mode of variability (explaining 50% of variability in both models) is the same as the regression signal of Figures 2c–2d. The second mode of variability (explaining 29% of variability) resembles the El Nino-La Nina pattern, which is symmetric about the equator as shown by *Lu et al.* [2008].

[8] After the separation of the variability into multidecadal and inter-annual/decadal using a 16-year Butterworth filter, a similar regression analysis, was performed to these two components of the variability. The results were similar, implying that this mode of atmospheric variability takes place both on multi-decadal and inter-annual time scales.

[9] Furthermore, in the all forcing GFDL simulations (in which 20th century atmospheric greenhouse gases, aerosols

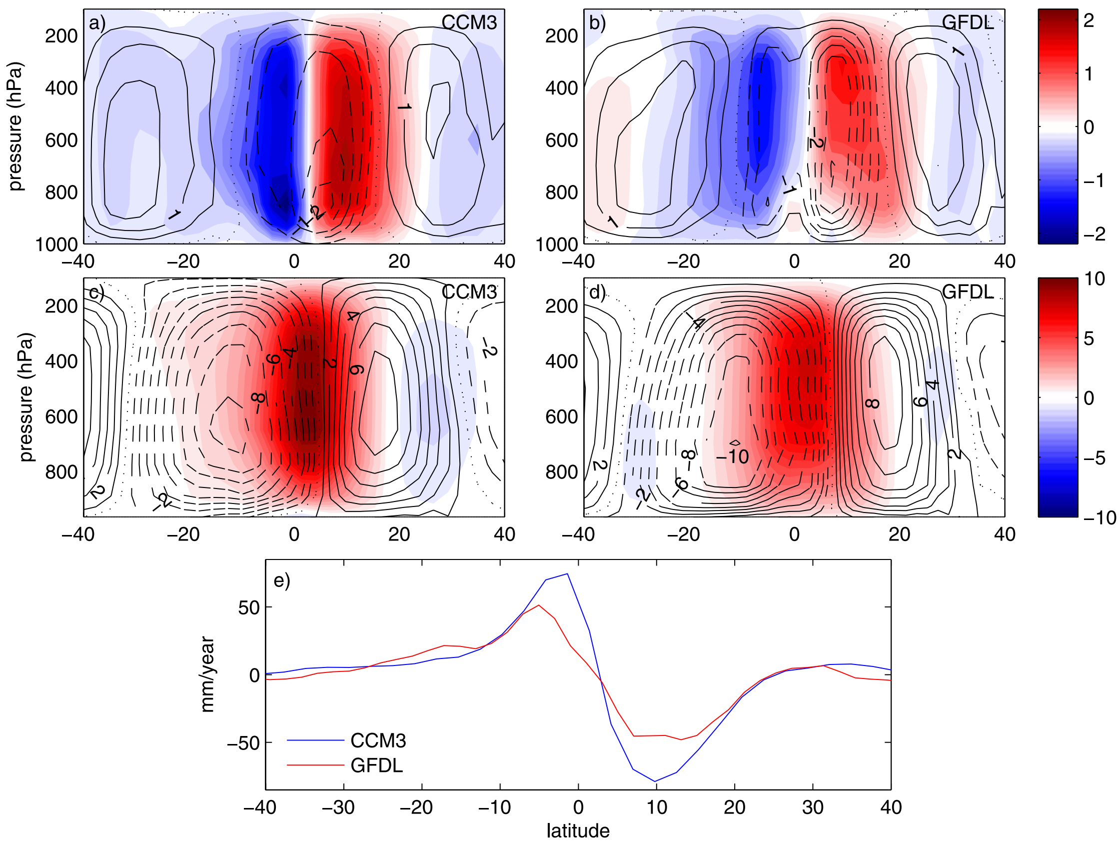

Figure 2. (a)–(b) Time average of the zonal mean ω-velocity (lines, 10^{-2} m/s units) and the regression of the ω-velocity anomaly on the normalized cross-equatorial V-index (colors, 10^{-3} m/s units), (c)–(d) time average of the zonal mean meridional streamfunction Ψ (lines, 10^{10} Kg/s units) and the regression of Ψ anomaly on the normalized V-index (colors, 10^{9} Kg/s units), and (e) regression of zonal mean precipitation anomaly on the normalized V-index. For the streamfunction, solid contours represent clockwise circulation, dashed contours represent counterclockwise circulation, and the dotted line represents the zero contour. The V-index was normalized with its standard deviation. Standard deviations for the V-index are 0.045 (GFDL) and 0.058 (CCM3). Only ensemble means are used, and results are multiplied with -1.

and solar variability are all included) the cross-equatorial meridional circulation as well as the atmospheric changes associated with it show a similar behavior (not displayed), which implies that this anti-symmetric signal is not directly driven by external forcing.

[10] The changes in the zonal mean meridional circulation are also associated with changes in the meridional heat transport. Figures 3a–3b show the regressions of the ocean and atmosphere meridional heat transport on the V-index. When there is anomalous northerly flow across the equator at the surface, the northward cross-equatorial atmospheric heat transport increases in both models. This anomalous heat transport in the atmosphere is balanced in part by an "implied" anomalous southward ocean heat transport (or reduced northward transport) that extends from 30S to 20N. There is little spread in this signal among ensemble members, as shown from Figure 3. We note that in an atmospheric GCM forced by SSTs, the surface energy budget is not closed, and the SSTs need not be consistent with the surface fluxes if the SST variability is being forced by the atmosphere, rather than the ocean. However, in this case, the regions of ocean heat divergence (convergence) are in fact regions of reduced (increased) SST, in both hemispheres, as shown in Figures 3a–3b. This is consistent with, but not proof of ocean driving of SST variability. North of 40°N and south of 40°S, however, this argument does not appear to hold, which may be attributed to the fact that, unlike in the tropical region, atmospheric heat transport has a much greater contribution in driving the SST changes compared to the ocean heat transport. Also, it has to be noted that in the calculation of the ocean heat transport for the CCM3 model, the latent heat of fusion due to snowmelt into the ocean, was not included. However, the contribution of this term to the results is small, confirmed from the calculations for the GFDL model.

[11] Furthermore, the V-index is highly correlated with the inter-hemispheric SST contrast (Figure 1c) with a correlation coefficient of 0.7 and 0.6 (both significant at the 99% confidence level) for the CCM3 and GFDL models, respectively. A more familiar index that can influence the inter-hemispheric gradient is the AMO (Atlantic Multi-decadal Oscillation), but that is less correlated with the V-index (0.48 and 0.24 for the CCM3 and GFDL models respectively, though these are still significant at the 99% level). These results indicate that it is not the SSTs in only one basin that influence the inter-hemispheric SST contrast and the cross-equatorial circulation, but rather the global SSTs, even though it should be noted that the multi-decadal

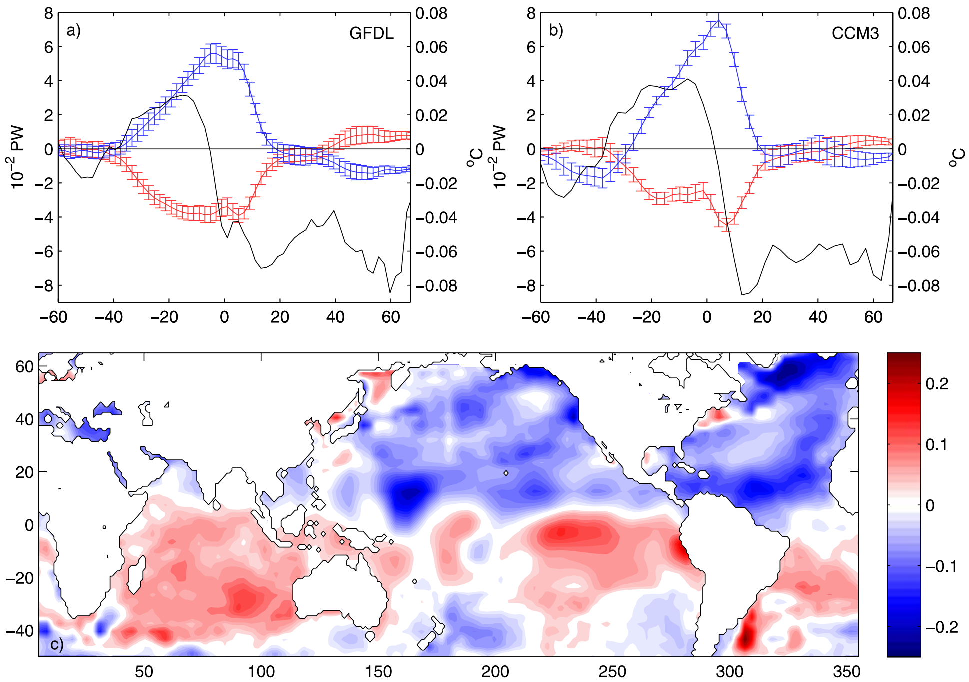

Figure 3. (a)–(b) Regressions of the anomalous heat transport for the ocean (red), atmosphere (blue), with one standard deviation ensemble member spread, and the zonal mean SST anomaly (black) on the normalized V-index. (c) Spatial distribution of the regression of the SST's on the normalized V-index (CCM3 model only). Results are multiplied with −1.

component of the inter-hemispheric SST difference of the individual basins may have different physical causes. This is illustrated in Figure 3c, with the regression of global SST on the V-index. This shows that when there is anomalous northerly flow across the equator, the SSTs in almost the entire Northern Hemisphere are colder than normal, and in the Southern Hemisphere, there is anomalous warmth throughout all three basins.

4. Discussion and Conclusions

[12] We study the change in the zonal mean atmospheric circulation in response to 20th century SST forcing. The results can be summarized as follows: The zonal mean cross-equatorial meridional wind is driven by the inter-hemispheric SST contrast, which comes about from correlated SST variability in all three basins. The cross-equatorial wind anomaly is associated with a displacement of the ITCZ toward the warmer hemisphere and the development of an anomalous overturning circulation in the tropics. This anomaly in the atmospheric circulation is also associated with an anomalous northward atmospheric heat transport that is partially compensating for an implied southward ocean heat transport. This mode of variability in the tropical atmosphere takes place both on multi-decadal and inter-annual time scales.

[13] Using the GFDL coupled model, *Zhang and Delworth* [2005] showed that a large reduction in the Atlantic thermohaline circulation, due to fresh water flooding of the North Atlantic, leads to a reduction in the northward ocean heat transport, by 0.5PW, and a SST cooling throughout the Northern Hemisphere. This change in the ocean shifts the ITCZ to the south, strengthens the Hadley cell, and increases the northward atmospheric heat transport, by 0.4PW, in order to compensate the reduction in the ocean heat transport. These anomalies were the result of an almost complete shutdown of the thermohaline circulation, and are ten and six times greater compared to the ocean and atmosphere heat transport anomalies, respectively, of our experiments, which are forced by 20th century SST. However, the Hadley circulation anomalies shown here are 30 and 24% of that of *Zhang and Delworth* [2005], for the CCM3 and GFDL model, respectively, suggesting that the cross-equatorial atmospheric circulation is quite sensitive to this kind of perturbation. We note that, unlike in *Zhang and Delworth*'s [2005] experiments, in the experiments shown here there is not full compensation between the ocean and the atmosphere heat transport at all latitudes.

[14] *Broccoli et al.* [2006] found a similar result, using a slab ocean coupled model forced with a relatively large asymmetry in the high latitude surface heat flux. In this case the atmospheric heat transport anomaly extended in both hemispheres from the equator to the high extra-tropics, implying an intensification of the tropical overturning circulation and the extra-tropical circulation as well. In a similar experiment, *Kang et al.* [2008] found that the tropical atmospheric response is sensitive to the convective scheme parameter that controls dry air entrainment in convective plumes. This suggests that cloud feedbacks are important, but the fact that they are not very robust from model to model, implies that the detailed tropical atmospheric response would differ, even if forced by the same anomalous ''implied'' oceanic heat transport. The difference in the cloud parameterization scheme between the two models we used (CCM3 and GFDL) could also be responsible for the difference in the magnitude of the response between the two models. Also we note, that the experiments mentioned above produced very large atmospheric

responses (heat transport anomalies of 1 to 4PW). In summary, all studies suggest that the southward displacement of the ITCZ is not locally, but globally forced by thermal or radiative forcing.

[15] Also of note, the change in the circulation associated with the V-index, also appears in the Northern Hadley cell strength index, defined as by *Oort and Yienger* [1996] as the maximum of the zonal mean meridional streamfunction, but with the opposite sign (not shown). This is consistent with the intensification of the Northern Hadley cell seen in reanalysis products over the last decades [*Quan et al.*, 2004; *Tanaka et al.*, 2004; *Mitas and Clement*, 2005], even though the reliability of these trends was questioned by *Mitas and Clement* [2006]. These previous studies did not identify the cause of the trend, but the analysis performed here indicates that the strengthening can be explained as the response to observed changes in the inter-hemispheric SST gradient. By covering a longer time period, our analysis shows that a comparable weakening of the cell occurred earlier in the century from around 1910 to 1960. These findings suggest that the simulated mean meridional circulation in the tropics does not appear to be as sensitive to the mean global warming that has occurred over the period of study as it is to the inter-hemispheric SST gradient. As a result, the linear trends of the surface cross-equatorial circulation over the 20th century are not distinguishable from zero. Also, the poleward migration of the northern boundaries of both southern and northern Hadley cell and the subtropical dry region, revealed in observation based studies [*Hu and Fu*, 2007] and coupled model based studies [*Lu et al.*, 2007], does not seem to be related with the multidecadal oscillation of the cross-equatorial meridional wind, as seen from the small changes of the circulation and the precipitation in the subtropics.

[16] **Acknowledgments.** The author is grateful to Naomi Naik for providing the CCM3 results, as well as Isaac Held and Tom Delworth for providing the GFDL results. Special thanks to Isaac Held for his useful comments on this paper. This work was funded by a NOAA Office of Global Programs grant (NA060AR4310142). CCM3 data were downloaded from http://kage.ldeo.columbia.edu:81/SOURCES/.LDEO/.ClimateGroup/.PROJECTS/.CCM3/.goga_new/.runs/.

References

Broccoli, A. J., K. A. Dahl, and R. J. Stouffer (2006), Response of the ITCZ to Northern Hemisphere cooling, *Geophys. Res. Lett.*, *33*, L01702, doi:10.1029/2005GL024546.

Chiang, J. C. H., and C. M. Bitz (2005), Influence of high latitude ice cover on the marine Intertropical Convergence Zone, *Clim. Dyn.*, *25*, 477–496.

Chiang, J. C. H., M. Biasutti, and D. S. Battisti (2003), Sensitivity of the Atlantic Intertropical Convergence Zone to Last Glacial Maximum boundary conditions, *Paleoceanography*, *18*(4), 1094, doi:10.1029/2003PA000916.

Hu, Y., and Q. Fu (2007), Observed poleward expansion of the Hadley circulation since 1979, *Atmos. Chem. Phys.*, *7*, 5229–5236.

Kalnay, E., et al. (1996), The NCEP/NCAR 40-year reanalysis project, *Bull. Am. Meteorol. Soc.*, *77*, 437–471.

Kang, M. S., I. M. Held, D. M. W. Frierson, and M. Zhao (2008), The response of the ITCZ to extratropical thermal forcing: Idealized slab-ocean experiments with a GCM, *J. Clim.*, *21*, 3521–3532.

Kiehl, J. T., J. J. Hack, G. B. Bonan, B. A. Bovile, D. L. Williamson, and P. J. Rasch (1998), The National Center for Atmospheric Research Community Climate Model: CCM3, *J. Clim.*, *11*, 1131–1149.

Lu, J., G. A. Vecchi, and T. Reichler (2007), Expansion of the Hadley cell under global warming, *Geophys. Res. Lett.*, *34*, L06805, doi:10.1029/2006GL028443.

Lu, J., G. Chen, and D. M. Frierson (2008), Response of the zonal mean atmospheric circulation to El Nino versus global warming, *J. Clim.*, *21*, 5835–5851.

Mitas, M. C., and A. Clement (2005), Has the Hadley cell been strengthening in recent decades?, *Geophys. Res. Lett.*, *32*, L03809, doi:10.1029/2004GL021765.

Mitas, M. C., and A. Clement (2006), Recent behavior of the Hadley cell and tropical thermodynamics in climate models and reanalyses, *Geophys. Res. Lett.*, *33*, L01810, doi:10.1029/2005GL024406.

Oort, A. H., and J. J. Yienger (1996), Observed interannual variability in the Hadley circulation and its connection to ENSO, *J. Clim.*, *9*, 2751–2767.

Quan, X.-W., H. F. Diaz, and M. P. Hoerling (2004), Change in the tropical Hadley cell since 1950, in *The Hadley Circulation: Past, Present, and Future*, edited by H. F. Diaz and R. S. Bradley, Cambridge Univ. Press, Cambridge, U. K.

Seager, R., Y. Kushnir, C. Herweijer, N. Naik, and J. Velez (2005), Modeling of tropical forcing of persistent droughts and pluvials over western North America: 1856–2000, *J. Clim.*, *18*, 4065–4088.

Tanaka, H. L., N. Ishizaki, and A. Kitoh (2004), Trend and interannual variability of Walker, monsoon and Hadley circulations defined by velocity potential in the upper troposphere, *Tellus, Ser. A*, *56*, 250–269.

The GFDL Global Atmospheric Model Development Team (2004), The new GFDL global atmosphere and land model AM2–LM2: Evaluation with prescribed SST simulations, *J. Clim.*, *17*, 4641–4673.

Trenberth, E. K., and J. M. Caron (2001), Estimates of meridional atmosphere and ocean heat transports, *J. Clim.*, *14*, 3433–3443.

Uppala, S., et al. (2004), ERA-40: ECMWF 45-year reanalysis of the global atmosphere and surface conditions 1957–2002, *ECMWF Newsl.*, *101*, 2–21.

Yoshimori, M., and A. J. Broccoli (2008), Equilibrium response of an atmosphere-mixed layer ocean model to different radiative forcing agents: Global and zonal mean response, *J. Clim.*, *21*, 4399–4423.

Zhang, R., and T. L. Delworth (2005), Simulated tropical response to a substantial weakening of the Atlantic thermohaline circulation, *J. Clim.*, *18*, 1853–1860.

A. C. Clement and D. F. Mantsis, Rosenstiel School of Marine and Atmospheric Sciences, University of Miami, Miami, FL 33139–1031, USA. (dmantsis@rsmas.miami.edu)